

10-12-1986

Matrix Effects in Secondary Ion Mass Spectrometric Analysis of Biological Tissue

Margaret S. Burns
University of California, Davis

David M. File
Naval Weapons Support Center

Vaughn Deline
Almaden Research Center

Pierre Galle
Faculty of Medicine

Follow this and additional works at: <https://digitalcommons.usu.edu/electron>

 Part of the [Life Sciences Commons](#)

Recommended Citation

Burns, Margaret S.; File, David M.; Deline, Vaughn; and Galle, Pierre (1986) "Matrix Effects in Secondary Ion Mass Spectrometric Analysis of Biological Tissue," *Scanning Electron Microscopy*. Vol. 1986 : No. 4 , Article 4.

Available at: <https://digitalcommons.usu.edu/electron/vol1986/iss4/4>

This Article is brought to you for free and open access by the Western Dairy Center at DigitalCommons@USU. It has been accepted for inclusion in Scanning Electron Microscopy by an authorized administrator of DigitalCommons@USU. For more information, please contact digitalcommons@usu.edu.



MATRIX EFFECTS IN SECONDARY ION MASS SPECTROMETRIC ANALYSIS
OF BIOLOGICAL TISSUE

Margaret S. Burns,*¹ David M. File,² Vaughn Deline,³ Pierre Galle⁴

¹Department of Ophthalmology, School of Medicine, University of California, Davis,
1603 Alhambra Boulevard, Sacramento, CA 95816

²Naval Weapons Support Center, Crane, IN 47522

³Charles Evans and Associates, Redwood City, CA 94063

³Current Address: IBM, Almaden Research Center, San Jose, CA 95120

⁴Department of Biophysics, Faculty of Medicine, 94010 Creteil, France

(Received for publication May 01, 1986, and in revised form October 12, 1986)

Abstract

We have made several observations during the course of our studies that show the presence of matrix effects in soft biological tissue and standards. The sputtering rate of gelatin is approximately twice that of epoxy resin, but the ion yield of lithium in gelatin is an order of magnitude less than in epoxy. Osmium impregnation of freeze-dried material significantly alters the localization of calcium, but not potassium and barium. The absolute count rate for calcium in osmicated tissue is increased several-fold above that in freeze-dried tissue. Scanning electron microscopy of sputtered material shows the formation of cones during sputtering, which is particularly, but not exclusively, associated with melanin granules and red blood cells. These structures are known to be highly emissive for Na, K, and Ca. Boron implanted tissue also exhibits selective boron emission from melanin granules. Relative proportions of monoatomic and polyatomic emission vary in epoxy, gelatin and tissue. Ion images of carbon, chlorine and vanadium in tissue embedded with a vanadium-doped epoxy resin show variations in local regions that correspond to tissue structure. The energy distributions of common secondary ions differed somewhat in resin and two different tissue regions.

These examples show the existence of potential matrix effects in soft biological tissue that involve both differential sputtering and ion yield effects.

KEY WORDS: Secondary Ion Mass Spectrometry, matrix effects, differential sputtering, biological tissue, quantitation, sputtering, energy distributions

*Address for correspondence:
Margaret S. Burns
Department of Ophthalmology
School of Medicine, University of California,
Davis, 1603 Alhambra Boulevard
Sacramento, CA 95816 Phone No. (916)453-5590

Introduction

The existence of "matrix effects" in secondary ion mass spectrometric analysis of materials has been well documented in a variety of systems (McHugh, 1975). These effects can be generally classified into two categories: 1) variations in the number of atoms physically removed (sputtered) under given conditions; and 2) variations in the number of secondary ions produced under given conditions. In other systems, these effects are known to be influenced, *inter alia*, by crystal orientation of the substrate, conductivity or insulation characteristics of the substrate, the concentration of the absorbed active primary ion species, the type of primary ions bombarding the target, and the range of the collision cascade, which is influenced by the atomic number and mass of the primary ion and target.

With regard to these characteristics, it has been suggested (Burns, 1982) that soft biological tissue might have advantageous characteristics for SIMS analysis. It contains a high oxygen content and under conditions of primary oxygen bombardment should produce an oxygenated surface environment, which is known to reduce variations in secondary ion yield. Crystalline material is not a common component of soft biological tissue. The matrix chemical composition of C, H, O and N is similar for all tissues. The most abundant elements of interest, Na and K, are present at normal concentrations between 10 and 140 mmol/kg, or ca. 400 to ca. 5500 ppm for K. Although there are density differences between subcellular organelles, the magnitude is not large. For example, membranes, being largely lipid, have a density of ca. 1.15 gm/cc, nuclei >1.30, and mitochondria 1.17, as measured by centrifugation (Rickwood, 1984). The same building blocks of protein, nucleic acids, lipids and carbohydrates are present in all cells, with the same range of chemical bonds - from C-H at 80 kcal/mole to C-O at 257 kcal/mole (CRC handbook, 1975). Thus, it did not seem surprising to be able to generate standard curves from protein and epoxy samples doped with added elements (Burns-Bellhorn and

File, 1979) or to apply this to quantitative SIMS analysis of normal and cataractous rat lenses (Burns and File, 1986).

However, the presence of matrix effects of variations in sputtering and in ion yield have been noted. Quettier and Quintana (1979) showed differences in emission of carbon in organic and inorganic matrices and attributed this to differences in ion yield. Farmer et al., (1981) showed preferential sputtering of heterochromatin and the Z-lines of muscle in both heavy metal stained and unstained frog skeletal muscle. Patkin et al., (1982) used "burn-through" images of ca. 0.5 μm sections of root tip fixed in glutaraldehyde and osmium to make corrections of ion images for differential sputtering. An excellent review of differential sputtering (Linton et al., 1982) and its impact on ion image formation also showed etch-resistant nucleoli in monolayers of cells.

During the course of our studies on SIMS analysis of biological tissue, we have made some observations which indicate the existence of matrix effects in soft biological tissue, most readily apparent in tissues that are heterogeneous with respect to cell type and morphology. In addition, studies with simple model systems also indicate the presence of matrix effects which must be taken into account in analysis of biological tissue.

Materials and Methods

Sputtering and Ionization Studies

Sputtering studies were performed on the Cameca IMS 300, using a primary beam of positively charged oxygen of 30 nA current, rastered over an area nominally 300 μm^2 . The total sputtering time, and the time required to sputter through the Au overcoating were monitored in seconds. The total depth of sputtering was measured with a Dek-Tak profilometer, and the dimensions of the sputtered area were measured with a Nikon microscope using a reticule in the eyepiece. Positive secondary ions were monitored from an area 30 μm in diameter in the center of the sputtered crater. Epoxy resin and gelatin standards of the elements of interest were prepared as previously described (Burns-Bellhorn and File, 1979), on silicon wafers and overcoated with 99.999% Au (Ernest F. Fullam, Inc., Schenectady, NY) using a Denton Vacuum Evaporator. Density determinations were made by direct weight measurements and volume measured by displacement of an appropriate solvent (water for epoxy resin and oil for gelatin films), and was 1.20 gm/cc for epoxy and 1.04 gm/cc for gelatin. Elemental analysis of epoxy resins was performed by Schwarzkopf Analytical Laboratories, Woodside, NY.

Estimates of the thickness of the gold layer were made on selected samples by assuming that the sputtered areas were the same, that sputtering through the gold is done at a constant rate and sputtering through the substrate is also a constant, for the given ion

current density. Then the sputtering speed, R, through the substrate is

$$R = (D_t - D_g)/(T_t - T_g) \quad (1)$$

where D_t is the total sputtered depth, D_g the thickness of the gold layer, T_t the total sputtering time and T_g the time to sputter through the gold layer. By using known values for 2 or more craters on the same sample, with different sputter times, and assuming R to remain constant, the depth of the gold layer can be calculated. This was 607 Å for an epoxy sample and 405 Å for a gelatin sample, not far from the estimated 500 Å Au coating.

The sputter rate, S_R , is here defined as the thickness of material removed in Angstroms per second for a given current density in picoamperes per μm^2 , i.e.

$$S_R = R/(I_p/A_s) = (d'/T)/(I_p/A_s) \quad (2)$$

where d' is the total sputtering depth (Angstroms) minus the gold coating, T the sputter time for the substrate alone (sec), I_p the primary ion current (picoamperes), and A_s the sputtered area in μm^2 .

Since our ultimate goal was to compare the ions detected of a given element, E, to sputtered atoms of this element, we calculated an apparent sputter yield, S, for only the element of interest, defined as the number of E atoms sputtered per unit area per second, S_E , divided by primary current density, J_i . We have

$$S_E = C(10^{-6})n_s d' N_0 / W_E T' A_s \quad (3)$$

where C is the concentration of element E in ppm; n_s is the density of the substrate in grams/ μm^3 ; W_E is the atomic weight of the atom; N_0 is Avogadro's number (6.03×10^{23} atoms/mole); and the other symbols are as above.

The incident ion density, in ions per unit area per second, is

$$J_i = I_p (0.624 \times 10^7 \text{ ions/coulomb}) / A_s \quad (4)$$

where I_p and A_s are defined above and it is assumed that the primary ion carries a single charge. Hence the ratio S_E/J_i , or "apparent sputter yield", is

$$S = 9.66 \times 10^{10} (C n_s d') / (W_E T' I_p) \quad (5)$$

The "apparent ion yield", I, is the number of secondary ions detected in a unit area divided by the number of primary ions incident on that area. The number of detected ions per unit area per second is

$$J_c = N_i / (3.14 d^2/4) \quad (6)$$

where N_i is the secondary ion count per second and d the diameter of the circle over which the secondary ions are counted. Hence

$$I = J_c/J_i \quad \text{or} \quad (7)$$

$$I = (2.04 \times 10^{-7})(N_i A_s / I_p d^2) \quad (8)$$

with A_s and d^2 in μm^2 and I_p in picoamperes. In our experiments $d = 30 \mu\text{m}$, and consequently

$$I = (2.27 \times 10^{-10}) N_i A_s / I_p \quad (9)$$

The ratio of I/S is equivalent to the useful ion yield, or ions detected per sputtered atom.

Osmium Studies

To see if there was an effect of the presence of osmium on the ion image formation, pieces of freeze-dried cat retina (Burns, et al., 1981) were suspended in osmium vapor for several hours, and then dry embedded in epoxy resin. An adjacent area of freeze-dried tissue was directly embedded in resin without osmium treatment. 10 μm thick sections were dry cut, overcoated with 99.999% gold, and then imaged in the IMS300 as previously described (Burns et al., 1981). In order to see if there was a qualitative effect on the sputtering process, following sputtering for a defined time period, the specimens were mounted on SEM stubs with silver paint, and the surface examined with a JSM 35 scanning electron microscope operated at 20 keV.

Boron Implantation

Boron implantation of 10 μm sections of epoxy embedded freeze dried retinal tissue was performed at Hughes Research Laboratories. Boron was implanted at 70 keV and a dose of 5×10^{13} ions/cm². Images of the tissue were taken on a Cameca IMS 3f using 100 nA primary current rastered over a 250 μm x 250 μm area.

Mass Spectra

Mass spectra were taken up to mass 300 on the Cameca IMS300 on resin and gelatin standards doped with calcium and barium and from tissue (retina) areas known to be rich in these two elements. The major peaks of calcium and barium were measured, as well as polyatomic species known to contain these elements.

Ion Images

Ion images of freeze-dried cat retina embedded in epoxy resin containing vanadium were taken with the IMS300 using an O₂ primary ion beam of 30 nA rastered over an area 300 μm^2 . The time to generate each image is shown in the Figures.

Energy Distributions

The energy distribution of the emitted secondary ions were studied on the Cameca IMS 3f, using a positive oxygen primary beam at 100 nA rastered over a 250 μm x 250 μm area. The energy slit (located at crossover following the electrostatic analyzer) is closed to allow an energy pass band of a few volts. Then the accelerating voltage of the sample is ramped so that the secondary ion beam scans across the energy slit at crossover. The ions are then mass analyzed, collected and detected in the usual manner. Selected retinal areas of freeze-dried toad and cat retina embedded in epoxy resin were checked.

Results and Discussion

Sputtering and Ionization Studies

The sputtering rate of the epoxy resin standards was approximately half that of the gelatin standards (Table 1), despite the fact that their densities are quite similar (1.20 gm/cc for epoxy and 1.04 gm/cc for gelatin). Since there can be inaccuracy in the measurement of the primary ion current these numbers may not be accurate in an absolute sense but are useful for relative comparisons since the same instrumental and measurement conditions were used in all cases. The matrix chemical compositions of these standards (Table 2) are similar, as are the types of chemical bonds involved in both substrates. The major difference is that gelatin contains a significant amount of nitrogen, and epoxy does not. Sputtering with oxygen and nitrogen are both considered to be "reactive" sputtering, tending to diminish differences in ionization yields. The sputtering rate for tissue in epoxy resin is the same as that for resin

Table 1: Sputter Rate

	AU/sec	AU/sec
	pA/ μm^2	
Epoxy resin (n = 6)	22.01 ± 6.91	2.64 ± 0.89
Gelatin (n = 3)	36.57 ± 3.58	4.39 ± 0.43
Tissue in Epoxy (n = 2)	21.75	2.61
Au layer (n = 4)	17.28 ± 3.10	2.07 ± 0.37

Table 2: Chemical Composition of Materials

	Weight Percent				
	C	H	O	N	O + N
Epoxy resin ^a	60	7	32	-	32
Gelatin ^b	63	(7) ^d	16	14	30
Dextran ^b	47	(7) ^d	46	-	46
DNA ^b	43	(7) ^d	34	16	50
Stearic Acid ^b	82	(7) ^d	11	-	11
Lens ^c	51	7	(23) ^d	16	39

^aDetermined; ^bCalculated;

^cPhilipson (1969); ^dBy difference.

alone, which might be expected if the overall sputtering rate is controlled by the embedding material. The major element composition of the most common materials encountered in biological tissue is quite similar. This includes protein (gelatin), polysaccharides (dextran), nuclear material (DNA) and lipid (stearic acid was used as an example). These also are similar to a simple tissue, ocular lens.

The comparison of ionization of different elements embedded in epoxy resin is shown in Table 3. The blank levels of lithium in resin and gelatin were 0. The calculation of ions detected over sputtered atoms shows the expected order of $Li > Ca > V > C$, based on the ionization probability for formation of a positive ion. However, comparing this figure for lithium in epoxy resin and lithium in gelatin shows a 10 fold difference in the lithium ions detected/sputtered atom, despite the fact that gelatin has a higher sputter rate than epoxy resin. Repeated measurements to confirm this effect would be helpful. The apparent ion yield for carbon in epoxy and carbon in epoxy containing tissue is similar. Calcium is a normal component of gelatin at fairly high levels (Burns-Bellhorn and File, 1979) and cannot be removed even by prolonged dialysis (unpublished results), therefore calcium was not included in these studies. At the time they were done we did not have vanadium containing gelatin samples.

Since the elemental composition of the matrix is similar for both epoxy resin and gelatin, and since the chemical bonding involved in both types of polymer are similar, and the density of the materials is not appreciably different, it is not obvious why the sputtering rate for

gelatin should be measurably greater than that of epoxy and the number of secondary lithium ions detected/sputtered atom be less in gelatin than epoxy resin. Under the conditions of oxygen bombardment and high substrate oxygen and nitrogen content, the differences in matrix effects should be minimized, unless the surface oxygen content is not saturated, but

Figure 1a to c. Freeze-dried, unosmicated tissue.

Figure 1d to f. Freeze-dried retina exposed to osmium vapor.

1a. Potassium emits from the melanin granules of the retinal pigment epithelium (RPE) and choroid (C) and somewhat from the outer nuclear layer (ONL).

1b. In freeze-dried tissue, calcium emits from the melanin granules of the choroid (C), the rod inner segments (RIS) but not the outer nuclear layer (ONL).

1c. Barium is emissive only from the melanin granules of the choroid (C).

1d. The potassium image in osmicated tissue follows the same pattern as non-osmicated with emission from the RPE, choroid (C), and outer nuclear layer (ONL).

1e. In osmicated tissue the calcium still emits strongly from the choroidal melanin granules (C), but now is emissive from the outer nuclear layer (ONL).

1f. The barium emits only from the choroidal melanin granules (C).

Magnification marker for all pictures = 20 μ m.

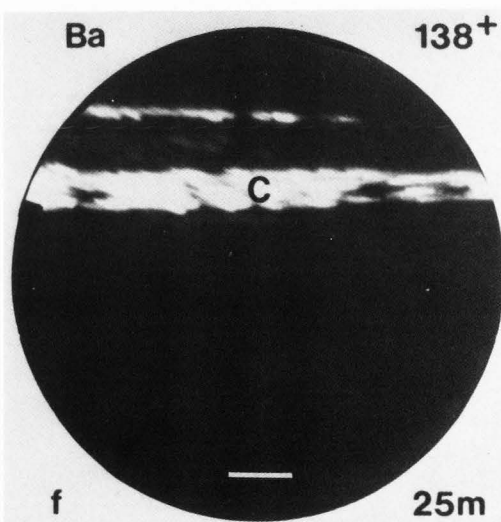
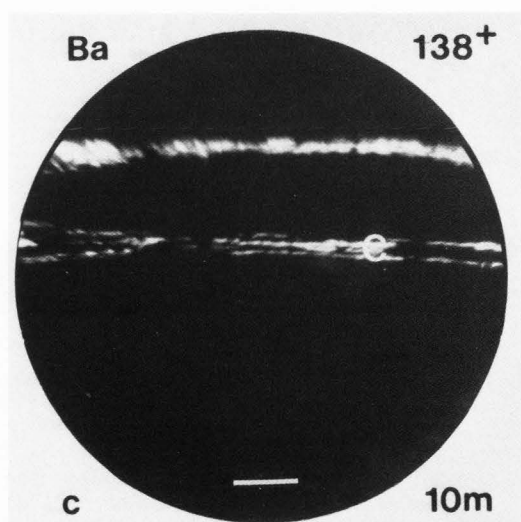
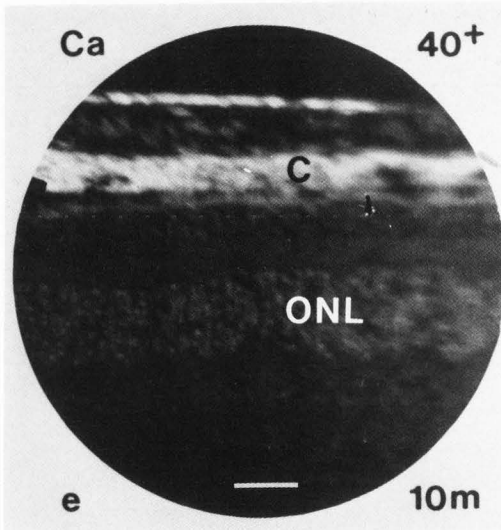
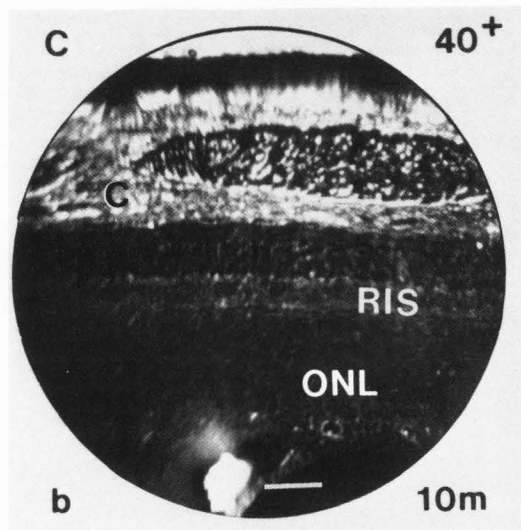
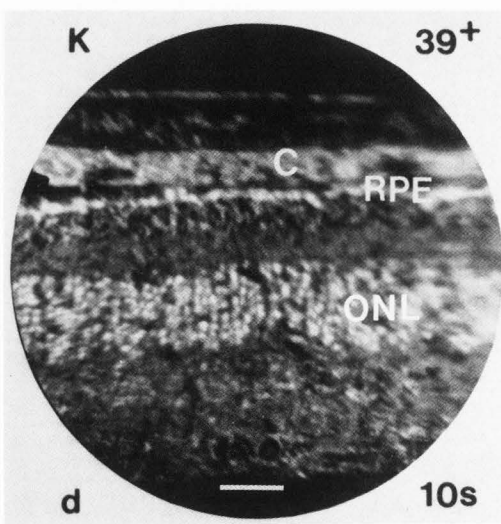
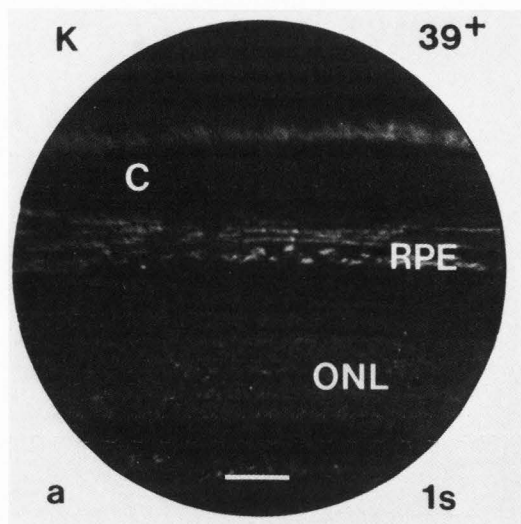
Table 3: Sputtering and Ionization

	Apparent Sputter Yield, S ^a	Apparent Ion Yield, I ^b	I/S ^c
Epoxy resin			
Li	2.16 x 10 ⁻² (2) ^d	3.35 x 10 ⁻⁵	1.60 x 10 ⁻³
Ca	6.61 x 10 ⁻³ (3)	2.24 x 10 ⁻⁶ (2)	4.28 x 10 ⁻⁴
V	6.37 x 10 ⁻³ (3)	5.07 x 10 ⁻⁷ (3)	7.87 x 10 ⁻⁵
C	12.14 (5)	5.85 x 10 ⁻⁷ (5)	5.14 x 10 ⁻⁸
Epoxy + Tissue			
C		5.41 x 10 ⁻⁷ (3)	
Gelatin			
Li	4.95 x 10 ⁻² (3)	9.45 x 10 ⁻⁶	1.73 x 10 ⁻⁴

^aAtoms/incident ion. ^bIons/incident ion. ^cIons/sputtered atom.

^dNumbers in parentheses indicate number of measurements made.

SIMS Matrix Effects



differences in ionization are apparent for lithium, and possibly for other ions, in these substrates.

Chemical information can be obtained in SIMS experiments, but these are usually done by bombardment with noble gases under low ion fluence (static SIMS) conditions (Hercules, 1979), and not the dynamic SIMS bombardment used here. Differences in mass spectra for a number of pure biological molecules under dynamic SIMS sputtering has been reported (Burns et al., 1979) so perhaps there are differences in ionization processes of material that appear similar on a macro scale.

We have reported quantitative studies of diffusible ion localization in lens tissue, using epoxy standards, that agreed quite well with values for Na, K and Ca obtained by other techniques (Burns and File, 1986). The choice of standard was fortuitous since, had we used gelatin standards, our values would have been higher by an order of magnitude, if the behavior of lithium accurately reflects that for Na, K and Ca.

Osmium Studies

In freeze-dried, unosmicated cat retinal tissue, the ion images in Figure 1a to 1c are obtained. Potassium emits strongly from the pigmented layers of the choroid and retina and also from the nuclear layers of the retina. Calcium emission is also high from the pigmented layers, but is weakest in the nuclear layer. Barium is found in the pigment granules of the choroid, but not the retina. When freeze-dried retina has been treated with osmium vapor, the images in Figure 1d to 1f are obtained. The potassium emission is still highest from the pigment granules and nuclear layers. The calcium emits from the pigment granules, but within the retina, the nuclear layers are now emissive. This is similar to images seen in glutaraldehyde and osmium fixed tissue (Burns, 1984). The barium localization is still confined to the choroidal pigment cells. This difference in calcium emission is also reflected in the total secondary ion current count rate (Table 4) in which total calcium counts of retina are more than 10 times higher in tissue which is fixed with glutaraldehyde and osmium compared to freeze-dried material. The potassium count rate is clearly less in dehydrated as compared to lyophilized material, as expected for a diffusible element (Stika et al., 1980).


The explanation that redistribution of elements occurs during treatment with osmium vapor appears not to be applicable since both the potassium and barium image remain constant before and after exposure to osmium, but the calcium image changes appreciably. Although rehydration of tissue is known to cause, occasionally, redistribution of calcium, where the calcium is precipitated onto structures that do not contain much Ca *in vivo*, but have intrinsic calcium binding capacity. However, redistribution of elements cannot account for an increase in total secondary ion count rate, unless there is a change in the ionization probability for this element. The solutions used for tissue processing did not contain

Table 4: Total Count Rate in Retina

	Amperes	
	K ⁺ , 39 ⁺	Ca ⁺ , 40 ⁺
Freeze-dried (n=7)	148 x 10 ⁻¹⁵	1.3 x 10 ⁻¹⁵
Glutaraldehyde and Osmium fixed, Dehydrated (n=6)	3.7 x 10 ⁻¹⁵	19.0 x 10 ⁻¹⁵

calcium, as determined by atomic absorption analysis. Although a loss of elements could be expected from these treatments, as compared with freeze drying, as seen with potassium, an increase in actual concentration of elements is not possible. However, an increase in ion yield of calcium due to changes in the local chemical environment could bring about this apparent enhancement.

The surface topography after sputtering freeze-dried tissue and freeze-dried tissue subjected to osmium vapors was examined by scanning electron microscopy (Figure 2). The surface topography prior to sputtering is seen to contain "blunt asperities" (Kelly, 1979). Sputtering of both freeze-dried and osmicated tissue shows cone formation that corresponds to the presence of melanin granules and red blood cells (Figure 2c and 2d). Qualitatively, the extent of cone formation from these structures appears to be less in freeze-dried, as compared to osmicated tissue. However, the freeze-dried retinal tissue is otherwise relatively free of cone formation, but the osmicated tissue exhibits cone formation throughout (Figure 2e and 2f). The extent of cone formation increases with increased sputtering time (Figure 3).

Figure 2a. Light micrograph of cat retina showing location of choroid (C), retinal pigment epithelium (RPE), and inner retinal edge (IN). Magnification marker = 20 μ m. 

2b. Scanning electron micrograph of unspattered surface at the level of the RPE, showing blunt asperities. Magnification marker = 5 μ m in this and subsequent frames.

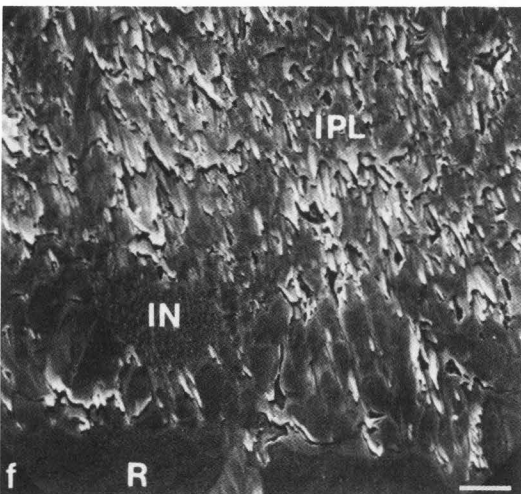
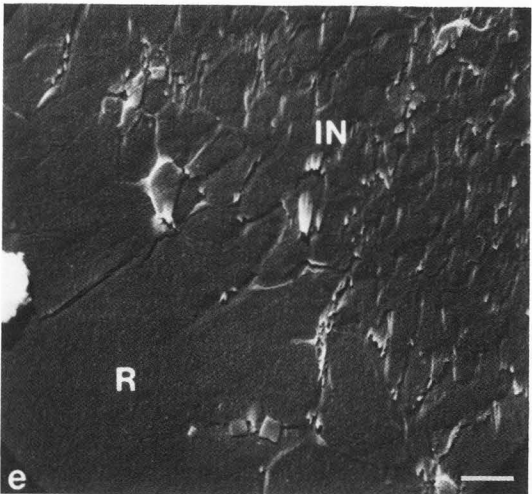
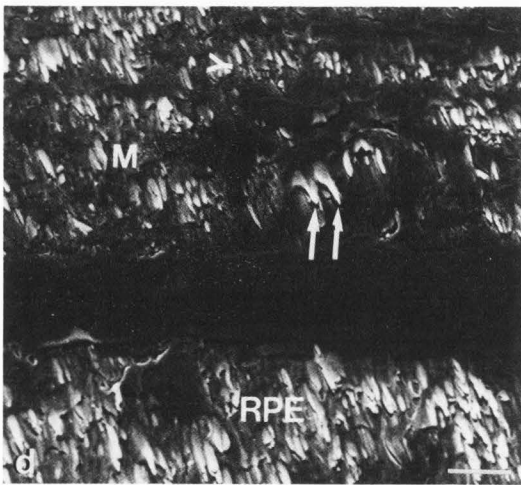
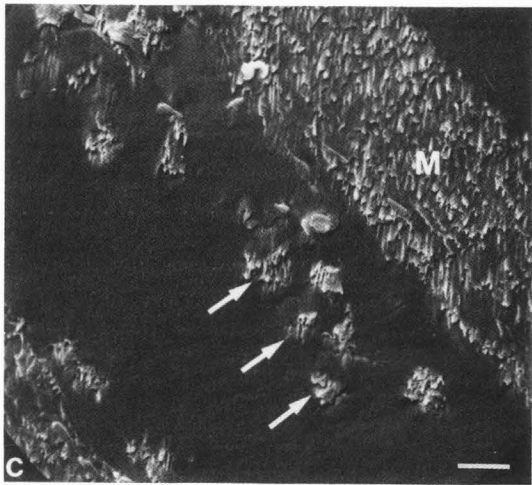
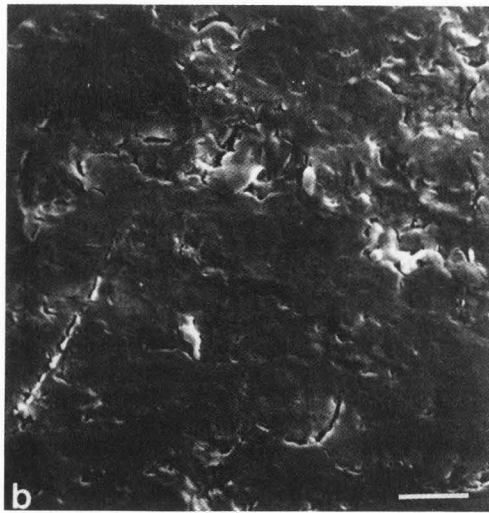
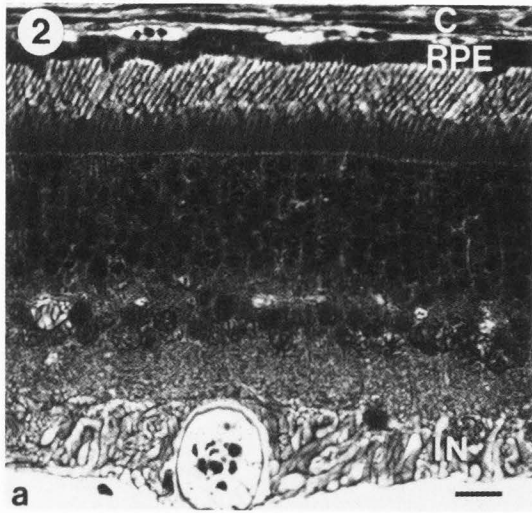
2c. Scanning electron micrograph of unosmicated tissue showing choroidal vessel with cone formation from red blood cells (arrows) and choroidal melanin containing cells (M).

2d. SEM of osmicated tissue showing emission from red blood cells (arrows) in small choroidal vessel and from melanocytes of choroid (M) and RPE.

2e. SEM of inner retinal edge (IN) and resin (R) of unosmicated tissue.

2f. SEM of inner retinal edge (IN) and resin (R) of osmicated tissue showing cone formation in the inner plexiform layer (IPL).

SIMS Matrix Effects



When retinal tissue is osmicated, the structures that appear to be most electron dense in the transmission electron microscope are melanin granules, red blood cells, lipid droplets and heterochromatin of the cell nucleus. Cell membranes also are osmiophilic, but the elaborate membranes of the rod outer segments are not made particularly dense with osmium alone. A correlation can be made with the osmiophilic structures and those that exhibit ready cone formation - melanin and red blood cells. We have also observed large lipid droplets in toad retina that do not sputter, as well as cone formation in nuclei of rod outer segments (not shown). But heavy metal content alone is not responsible for the etch resistance of these structures, as the unosmicated tissue showed qualitatively similar cone formation in melanin and red blood cells. Farmer et al., (1981) showed in muscle tissue that heterochromatin and the Z-band (which are both stained with heavy metals) were preferentially etched in both osmicated and unosmicated tissue. Adjacent structures that were also electron dense were not preferentially etched. Thus the presence of heavy metals alone does not indicate whether a structure will be preferentially etched or etch resistant. The association of these structures with uptake of heavy metals and specific etching effects suggests that there is a difference in the local chemical environment which may control both these phenomena, and potentially the ion yield of these microareas.

Of importance is the effect of etching on ion emission and the interpretation of emission as being related to concentration in ion images. Specifically, melanin granules from all tissues examined consistently show high emission of sodium, potassium, calcium and sometimes barium (Burns et al., 1981). Since cone formation effectively creates additional surface area for adsorption of the primary species and from which ions can be sputtered, it is possible that the intense emission seen from these structures overstates the actual elemental concentration present. We have made calculations of the calcium and barium content of pigment granules from counts taken in restricted areas and find the results to be much higher than that reported for isolated pigment granules. In any case, the assumption that a faster sputter rate is proportional to an increase in secondary ion intensity may not hold for all structures, and must be evaluated on a case by case basis (Patkin et al., 1982)

Boron Implantation

When boron was implanted into freeze-dried cat retinal tissue, the ion image of potassium was similar to that seen in previous studies (Figure 4). The boron emission was from the retinal and choroidal area containing melanin granules, as seen in the previous studies. This image persisted through taking four images during a total 33 minutes of sputtering which, at an average sputtering rate of 2.5 Angstroms/sec, reflects the removal of 0.5 μm of material.

One explanation for this result would be that boron was implanted unevenly into the tissue and was stopped nearer the surface in the melanin containing regions. This seems unlikely since the image persisted through a considerable depth of tissue, although cone formation in this region would result in loss of depth resolution and persistence of the boron image. Another explanation would be that the boron was preferentially ionized in the regions corresponding to the melanin granules, as discussed above for the ions naturally present. Whatever explanation is the correct one, it makes more difficult the application of ion implantation as an internal standard for quantitation procedures in biological tissue that is heterogeneous on a microscale (Harris et al., 1983).

Mass Spectra

The results of measuring the proportion of polyatomic species containing calcium or barium are shown in Tables 5 and 6. The count rate of the major isotope, 40^+ or 138^+ , are arbitrarily set at 100 and the count rate of the polyatomic species are given as a percent of that number. It can be seen that the major calcium polyatomic species, $CaOH^+$, varies from 12 to 26% depending upon the matrix material. Emission of the analogous $BaOH^+$

Table 5: Relative Proportion of Polyatomic Species

	<u>Resin</u>	<u>Gelatin</u>	<u>Tissue</u>
$40^+ Ca^+$	100.0	100.0	100
$57^+ CaOH^+$	12.0	26.0	16
$66^+ CaC_2H_2^+$ $CaCN^+$	0.2	7.0	6
$77^+ Ca^{37}Cl^+$	0.7	0.4	6

Table 6: Relative Proportion of Polyatomic Species

	<u>Resin</u>	<u>Gelatin</u>	<u>Tissue</u>
$138^+ Ba^+$	100.0	100	100
$155^+ BaOH^+$	7.0	22	22
$164^+ BaC_2H_2^+$ $BaCN^+$	0.7	24	18
$175^+ Ba^{37}Cl^+$	6.0	21	22

SIMS Matrix Effects

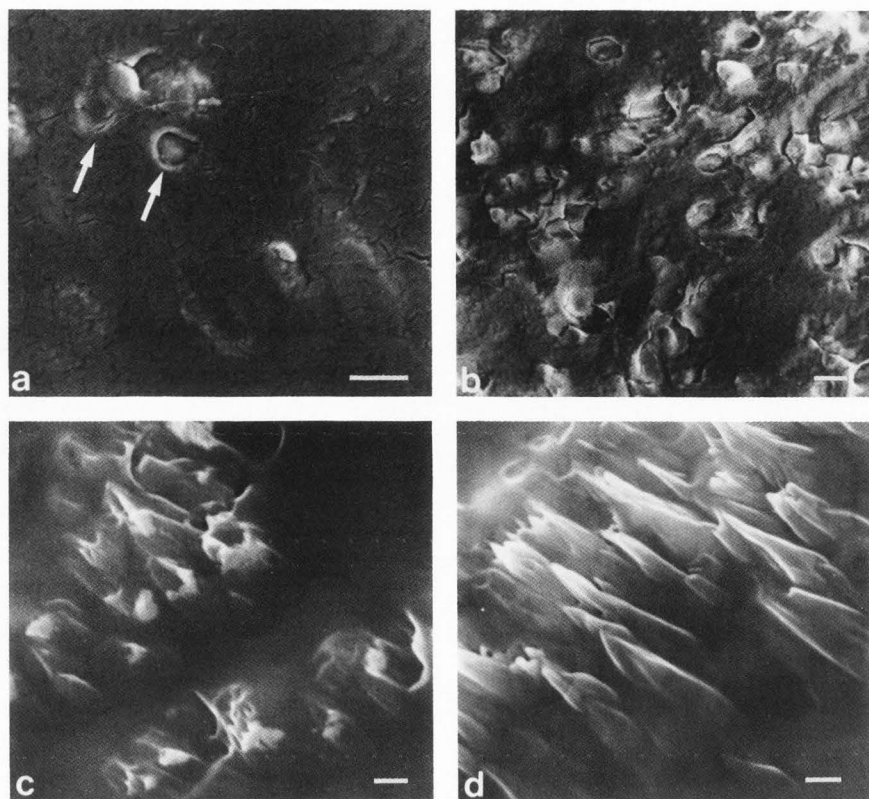


Figure 3. The extent of cone formation increases with time.

3a. Unspattered surface of osmicated toad retinal pigment epithelium cell showing blunt asperities (arrows) that seem to be melanin granules. Magnification marker = 10 μm in this and subsequent frames.

3b. An RPE cell after 5 minutes of sputtering.

3c. An RPE cell after 30 minutes of sputtering.

3d. An RPE cell after 60 minutes of sputtering. The ion dose in Figures 3b to d ranged from 2 to 28×10^{17} ions/cm².

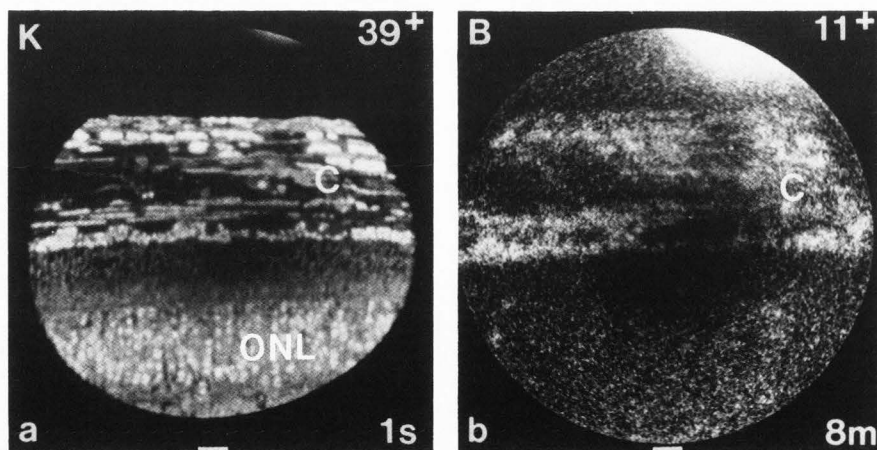


Figure 4a. Potassium image of osmicated cat retinal tissue with intense emission from choroidal melanin granules (C) and nuclei of outer nuclear layer (ONL). Magnification marker = 10 μm .

4b. Image of boron implanted into this tissue. Emission is seen most strongly from the choroidal melanin granules (C), in the same pattern observed for melanin. Magnification marker = 10 μm .

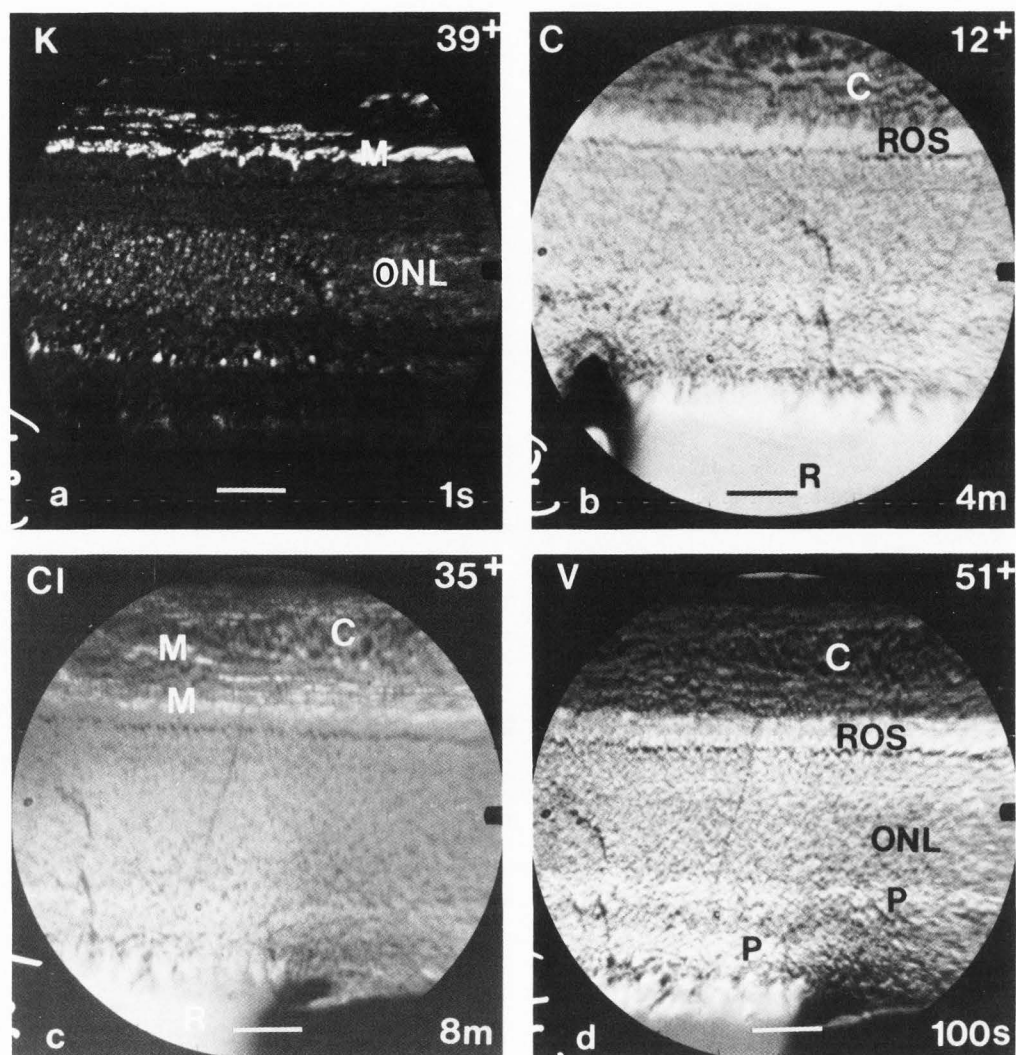


Figure 5a. Potassium image of freeze-dried, unossicated cat retina. Emission from the melanin granules (M) is intense and less so from the outer nuclear layer (ONL). Magnification marker = 20 μ m in this and subsequent frames.

5b. Carbon, 12^+ emission from the same area is not uniform and stronger from the rod outer segments (ROS) and resin (R) than from the choroidal region (C).

5c. Chlorine emission from freeze-dried, unossicated cat retinal tissue is high from the melanin granules (M) and resin (R), but less so from the extracellular space of the choroid (C).

5d. Vanadium emission from the same specimen as 5c. Vanadium is more emissive from the rod outer segments (ROS) and plexiform layers (P) than from the outer nuclear layer (ONL). It is low from the choroidal area (C).

ion also varies from 7 to 22%, but is less in resin and more in tissue than CaOH^+ . The higher molecular weight barium polyatomics comprise a greater proportion of the total barium counts than do the analogous calcium polyatomics. This difference in formation of polyatomic species also is dependent on the nature of the matrix used.

Ion Images

Ion images of carbon, chlorine, and vanadium from freeze-dried cat retina embedded in epoxy resin containing vanadium were examined (Figure 5). The image of carbon was expected to be

homogeneous throughout the tissue since the content of carbon is fairly constant in different types of biological materials (Table 2). However, the emission showed variation with cellular layers. It was higher in an area corresponding to the photoreceptor outer segments and diminished in the choroidal area, which is largely extracellular space. The chlorine image was expected to be uniform, since the epoxy resin contains a significant chlorine content. However, the chlorine showed some enhanced emission in areas corresponding to pigment granules of the choroid and retina.

The vanadium image reflected the general geography of the sample. It is not surprising that it is slightly less emissive from the nuclear layers, which are more closely packed than the plexiform layers and therefore would have less extracellular space to be filled by the embedding medium. But the choroid, which is largely extracellular space was the least emissive area. It appears that the presence of tissue is altering the ion emission of major matrix components. This could be because of different sputtering rates in different areas but if this were so we would expect the ion images of carbon, chlorine and vanadium to be similar. It seems more likely that the differing local chemical environment in the substrate, induced by the tissue, causes differing ion yields for these elements.

Energy Distributions

There were some differences in the secondary ion energy distributions from resin, retinal pigment epithelial area containing melanin granules, and inner retinal areas (Figure 6) of either toad or cat freeze-dried retina embedded in epoxy resin, although a consistent pattern was not observed. These differences in ion energy may be related to charging of the sample or variations in collection efficiency due to uneven topography in differing areas.

Summary

Several different lines of evidence show the existence of matrix effects and differential sputtering of heterogeneous soft biological tissue. The implication is that the local chemical environment controls both sputter rates and ionization rates of elements found in tissue, despite similar chemical compositions, densities, and bond energies in this material. Before quantitative analysis of localized regions at the micron and submicron range of heterogeneous material can be carried out, the variation of these effects will have to be incorporated into the analytical scheme used.

Acknowledgements

This work was supported in part by NIH Grant #EY05785, an unrestricted grant from Research to Prevent Blindness, and a Research Manpower Award to MSB.

We wish to thank Dr. Robert Wilson for ion implantation of samples, Ms. Ellie Morales for scanning electron microscopy, Annick Quettier for ion images, Henry Oksman for sputtering studies and Jack Huneke, Robert K. Lewis and Charles A. Evans, Jr. for valuable discussions.

References

Brenna JT, Morrison GH. (1986). Ionization probability variations due to matrix in ion microscopic analysis of plastic-embedded and ashed biological specimens. *Anal. Chem.* **58**, 1675-1680.

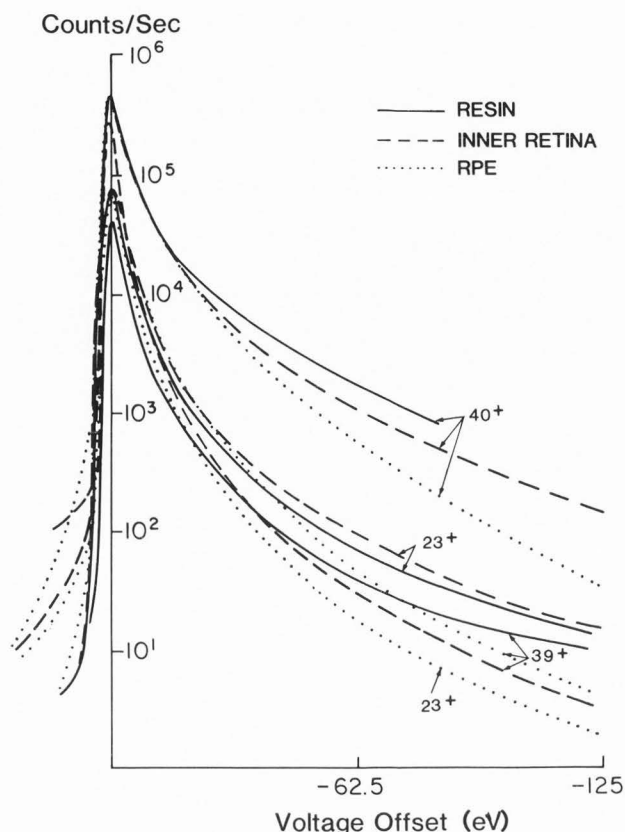


Figure 6. Energy distributions of sodium, 23⁺, potassium, 39⁺, and calcium, 40⁺, from doped resin, the melanin rich region of RPE, and inner retina.

Burns MS. (1982). Applications of secondary ion mass spectrometry (SIMS) in biological research: A review. *J. Microscopy* **127**, 237-258.

Burns MS. (1984). Secondary Ion Mass Spectrometry, in: *Analysis of Organic and Biological Surfaces*, P. Echlin (ed), John Wiley and Sons, NY, 259-283.

Burns MS, Levi-Setti R, Chabala J, Wang YL. (1986). High resolution scanning ion microprobe analysis of retinal tissue. In: *Microbeam Analysis - 1986*, A Romig and W Chambers (eds.), San Francisco Press, 107-108.

Burns MS and File DM. (1986). Quantitative microlocalization of diffusible ions in normal and galactose cataractous rat lens by secondary ion mass spectrometry. *J. Microscopy*. In Press.

Burns MS, File DM, Quettier A and Galle P. (1979). Comparison of spectra of biochemical compounds and tissue preparations. In: *SIMS II* (eds. A. Benninghoven, C.A. Evans, R.A. Powell, R. Shimizu, H.A. Storms) Springer-Verlag, NY, p. 259.

Discussion with Reviewers

Burns MS, File DM, Brown KT and Flaming DG. (1981). Localization of calcium and barium in toad retina by secondary ion mass spectrometry. *Brain Res.* 220: 173-178.

Burns-Bellhorn MS, File DM. (1979). Secondary ion mass spectrometry (SIMS) of standards for analysis of soft biological tissue. *Anal. Biochem.* 92, 213-221.

CRC Handbook of Chemistry and Physics (1975) CRC Press, Boca Raton, FL. pp. F-215-219.

Farmer ME, Linton RW, Ingram P, Sommer JR and Shelburne JD. (1981). Preferential sputtering effects in the ion microanalysis of biological tissues. *J. Microscopy.* 124: RP1-RP2.

Harris WC, Chandra S and Morrison GH. (1983). Ion implantation for quantitative ion microscopy of biological soft tissue. *Anal. Chem.* 55: 1959-1963.

Hercules DM. (1979). Analytical applications of SIMS. In: SIMS II (eds. A. Benninghoven, C.A. Evans, R.A. Powell, R. Shimizu, H.A. Storms) Springer-Verlag, NY, pp. 122-126.

Kelly R. (1979). Basic aspects in the sputtering of atoms, ions and excited states. In: SIMS II (eds. A. Benninghoven, C.A. Evans, R.A. Powell, R. Shimizu, H.A. Storms) Springer-Verlag, NY, pp. 21-25.

Linton RW, Farmer ME, Ingram P, Walker SR and Shelburne JD. (1982). Ion beam etching effects in biological microanalysis. *Scanning Electron Microsc.* 1982; III: 1191-1204.

McHugh JA. (1975). Secondary ion mass spectrometry. In *Methods of Surface Analysis* (ed. A.W. Czanderna), Elsevier, NY, pp. 223-278.

Patkin AJ, Chandra S and Morrison GH. (1982). Differential sputtering correction for ion microscopy with image depth profiling. *Anal. Chem.* 54, 2507-2510.

Philipson B. (1969). Distribution of protein within the normal rat lens. *Invest. Ophthalmol.* 8: 258-270.

Quettier A and Quintana C. (1979). Distinction between organic and inorganic carbon in calcium carbonate material by secondary ion mass spectrometry (SIMS). *Compt. Rend. Acad. Sci. (Paris)* 289: 433-440.

Rickwood D. (1984). *Centrifugation: A Practical Approach.* IRL Press, Washington.

Stika KM, Bielat KL and Morrison GH. (1980). Diffusible ion localization by ion microscopy: A comparison of chemically prepared and fast-frozen, freeze-dried, unfixed liver sections. *J. Microscopy* 118: 409-420.

R.W. Linton: Couldn't the possible difference in molecular weight distributions of the epoxy vs. gelatin polymers explain different sputtering rates?

R. Levi-Setti: Concerning the overall sputtering rates of gelatin, substantially higher than that of epoxy resin, in spite of similar densities and chemical composition, the presence of nitrogen in gelatin may provide a clue. This in fact will open a channel for the emission of CN⁻, which we know is very intense for all protein containing materials, and such a channel is not available for epoxy.

Authors: Both of these suggestions concerning the differences in sputtering rate between two similar materials are interesting. We have no information on the sizes of the final polymers in these two materials and so do not know how to ascertain if this plays a part in the observed differences. Certainly, the presence of nitrogen in gelatin (and tissue) gives a strong CN⁻ signal, which could account for some of the difference in sputtering rate of gelatin compared to epoxy, but then we would have expected a higher rate for tissue than epoxy.

D.S. Simons: Could the difference in ion yield of lithium between epoxy and gelatin be caused by differences in ionic mobility of lithium in the two matrices coupled with a small amount of surface charging? Are the results the same under negative oxygen bombardment?

A. Lodding: In Table 3 you show that the effective ionizability for Li is by about an order of magnitude higher in epoxy than in gelatin. You are speculating that a similar difference between the two matrices might also apply to the ionization of Ca, V and C. Can you give a physical reason why this should be so? Are you planning measurements to actually compare gelatin and epoxy with respect to other elements than Li?

A. Lodding: Lithium often has a strong tendency to combine with nitrogen. One difference between epoxy and gelatin is that the latter contains nitrogen. Have you checked the mass spectra for the possible occurrence of a LiN⁺ peak, which might encroach on the Li⁺ intensity? Table 5 shows no comparison including gelatin.

Authors: These questions all concern the differences in ion yield of lithium between epoxy and gelatin. It should be noted that more experiments need to be done to confirm this point. It is possible that there are differences in ionic mobility of lithium in the two matrices, in that gelatin has a net negative charge, and perhaps there are electrostatic interactions between the lithium ion and the charged side chains of collagen that do not exist with the epoxy polymer. We have not seen evidence of surface charging on a macro scale, but that does not rule out that it exists on a micro scale. We have not done studies with negative ion bombardment.

We did not mean to imply a similar ionization process for V and C, but would expect the physiologically important elements Na and K to behave similarly since they are atomically similar. Whether Ca and Mg, two other physiologically important elements behave similarly remains to be seen in future studies.

There is no LiN^+ peak at mass 21. Table 5 has been labelled to show that the protein used was, indeed, gelatin.

R. Levi-Setti: There are broad implications in regard to the observations of differential effects in the emission of specific monoatomic species. These may be the local manifestation of a much more complex set of interrelated phenomena. In very general terms, familiar to atomic, nuclear and particle physicists, interactions which may lead to a variety of final states are subject to a conservation law (unitarity) saying that the sum of all outgoing fluxes cannot exceed the ingoing flux of particles. This implies that a connection exists between the various possible final states or channels which are the outcome of the interaction. If new channels open up, this will reflect on the outgoing fluxes of all other channels. The description of these effects requires the use of a so-called multi-channel formalism. An hydrodynamical analog provides an intuitive picture here.

If we transpose this picture to the interaction volume involved in the sputtering process, the availability of different channels, (e.g. emission of cluster ions and molecules which may be matrix-dependent) cannot fail to affect the other channels (e.g. monoatomic emission.) Matters are complicated here by the fact that for each channel (atomic or molecular species), there are three subchannels i.e. positive, negative and neutral. Then in principle, one would expect that anomalies in the emission yields of specific species and charge states may be reconciled in a broader view of the emission process. Some channels may be wide enough to be little affected by the others, i.e., there may be standards much less sensitive than others to differential structural effects.

In any case, it would seem that quantification should benefit from the simultaneous observations and accounting of as many channels containing a particular element as possible, inclusive of polyatomic species as well as positive and negative ions.

Authors: Your perception of this problem is extremely valuable.

R. Levi-Setti: Why are the Cameca images always blurred and distorted at the periphery of the field of view? Is this due to aperture aberrations (coma, spherical aberration), to field aberrations (cushion, barrel), chromatic aberration or what?

Authors: None of us are qualified enough in ion optics to answer this question.

R. W. Linton: Lengths of exposures for ion images generally seem very long, for example 10 and 25 min. for Ca and Ba, respectively (Figure 1). Is a low speed film being used to improve image quality?

Authors: The exposures used on the Cameca IMS300 are generally longer than for the IMS 3f because the count rate at the fluorescent screen is about 100 times lower than at the channelplate of the IMS 3f. The intrinsically low background on the IMS300 improves the image quality, which was taken on Agfa film with a 400 ASA rating, pushed to 800 during development.

R.W. Linton: How were the spectral assignments of polyatomic species confirmed in Tables 5 and 6?

Authors: The assignments are made on the basis of the most probable species, given the limited elemental content of the material being examined. The positive ion spectra of biological material is quite simple with only a few major species. In the case of barium with 5 isotopes of appreciable abundance, a family of barium isotopes is seen for each polyatomic species, indicating a common component of the polyatom in addition to barium. For polyatomic species containing Cl, one sees a polyatom for both ^{35}Cl and ^{37}Cl . We did not, at the time these studies were done, have the capability of doing high resolution mass spectra.

R.W. Linton: How were the sputtered structures confirmed to be red blood cells in Figure 2c,d? Were these cells examined by SEM prior to ion bombardment?

Authors: An adjacent light microscopic section is always used as a guideline to the area examined by SIMS for general tissue patterns. Since the cells mentioned are inside a large blood vessel (Figure 2c) or a choroidal capillary (Figure 2d), known from pattern recognition and years of experience looking at retinal morphology, they are clearly blood borne cells. Although they might be platelets or leucocytes, these cells are rather rare in normal tissue, and the most likely candidates are red blood cells.

D.S. Simons: Are you aware of any studies in biological matrices where oxygen gas flooding has been combined with oxygen bombardment in an attempt to minimize spatial variations in ion yield, as has been demonstrated in metal alloy systems?

Authors: To the best of our knowledge, such studies have not been done.

D.S. Simons: What procedures would you recommend for carrying out quantitative analysis of a specific cation in soft biological tissue, given the complicating effects reported here?

Authors: The approach for absolute quantitation studies explored by Brenna and Morrison (1986) may turn out to yield excellent

results, although, as these authors point out, it may be tedious and then the question will be if the investment is worth the outcome.

An alternative is asking, as many biological questions do, only for relative values could be approached by comparing local ion content for the same or similar ions under two different experimental protocols. The inherent assumption would be that variations in sputtering and ionization would be the same for each element in the same tissue area, which itself would need to be tested. Galle (personal communication) has used this approach to good effect in looking at isotopes of iodine in thyroid.

D.S. Simons: Would you comment on the observation made in Linton et al. (1982) that sputter resistance appears to be correlated with low water content in certain cellular compartments?

Authors: When soft biological tissues are treated by any means to remove water without infiltration of substitute fluids, such as critical point drying or freeze-drying, the net effect is that diffusible components (either elements or proteins) condense on the nearest structurally stable forms, whatever this may be. Linton et al. (1982) observed this in frozen, freeze-dried cell monolayers. We have seen it in freeze-dried preparations of retina, especially the large choroidal vessels, in which condensation of plasma proteins within the lumen form Na and K rich strands in the freeze-dried material (Burns et al., 1986). Therefore, by difference, the structures originally low in water (such as the pigment granules discussed in this paper) become the most stable structural elements remaining in the preparation, with added accretions of diffusible ions. So it is possible that highly water-rich structures become spaces and the more structurally stable components appear etch resistant. It is premature to make a simplistic explanation, since the works of Linton et al (1982) and our own show anomalies. More work needs to be done on this point.

G.M. Roomans: Could you elaborate on your specimen preparation (freeze-drying, osmium post-fixation, and embedding) with respect to how you avoid rehydration of the tissue?

Authors: The freeze-drying is done in a chemical sorption system, in which the sample is kept at -30°C in a vacuum established by a temperature differential, with the zeolite adsorbent in another chamber in liquid nitrogen. Upon removal from the -30°C freezer, the material is allowed to warm to room temperature and then the vacuum is broken. The specimens are stored in desiccators over P_2O_5 until embedded in epoxy resin in a vacuum oven at 60°C . The osmium postfixation of freeze-dried material was carried out at room temperature by suspension of a piece of freeze-dried retina over solid osmium in a closed container at room temperature.

R.W. Linton: In the ion implantation study, why couldn't the B image persist through a considerable depth of tissue as a result of drastic loss of depth resolution associated with cone formation?

Authors: This explanation is equally viable and then necessitates the total consumption of a tissue slice and integration of total count rates for elements of interest and the implanted standard, and certainly complicates quantitation of biological tissue analysis by SIMS. This approach has recently been explored by Brenna and Morrison (1986).

A. Lodding: A look at the energy distribution curves in your Fig. 6 does in fact reveal rather significant slope differences between the different matrices. Shouldn't the distributions of ions from gelatin also be included? These matrix differences in energy distributions could result in considerable differences in ionizability factors, particularly if the secondary ion energy window is narrow (as in the Cameca IMS 300) or at relatively high offset voltages. What was your energy pass-band when you did the measurements on Li from gelatin versus epoxy?

Authors: Your questioning has caused us to reexamine our interpretation of the data. For example, the difference in integrated count rate of sodium in RPE and sodium in inner retina (the worst disparity) is approximately 30%. This could be due to local charging effects, or, equally to variations in transmission due to local fields at the sample surface caused by the uneven topography we have noted above. This question requires more study.

The measurements on Li^+ in gelatin vs. epoxy were done on the Cameca IMS300, and the detector was peaked on the mass prior to each determination. The energy window was opened as fully as possible, so all ions arriving at the detector were measured.